

Identifying and Tracking a Guide Wire in the Coronary Arteries During Angioplasty from X-Ray Images

Daphna Palti-Wasserman, Alfred M. Brukstein, and Rafael P. Beyar,* *Member, IEEE*

Abstract— During angioplasty, a guide wire (GW) is routinely placed in the coronary artery. Balloon inflation during angioplasty causes transient occlusion of the coronary artery and regional dysfunction. Thus, it is of major importance to monitor myocardial function, which may be impaired during this period. Since the GW moves with the coronary arteries, information regarding myocardial function can potentially be extracted from the GW motion. An algorithm is suggested which is a step toward such monitoring. The algorithm presented is a semiautomatic procedure for identifying and tracking the GW using specific characteristics of the GW. This algorithm is based on working in limited active windows. A preprocessing stage which enhances the GW by the use of a modified Laplacian filter or a modified Marr–Hildreth filter is introduced. The second stage of the algorithm is the tracking of the GW, which is based on fitting a second-degree polynomial to the GW using the Hough transform in each window. To further improve the results further modifications of the basic algorithms that were taken. A single set of parameters, which enabled good tracking for a large number of images taken during angioplasty, was fitted to the final algorithm.

Index Terms— Coronary angioplasty, guidewire, tracking, ventricular function, wall motion.

I. INTRODUCTION

CORONARY angioplasty is a routine procedure for treatment of coronary stenosis. Transient coronary occlusion during angioplasty typically causes abnormal function in the region supplied by the treated vessel due to transient ischemia [12], [20], [21]. It is, therefore, of clinical importance to be able to monitor the degree of abnormal function and its return to baseline during and between multiple balloon inflations of variable durations. A variety of methods, algorithms, and imaging devices, such as ventricular angiography [5], [29] and ultrasound imaging [34], may be used for detection of wall motion abnormalities in the catheterization laboratory. However, neither of them can be easily and routinely used

during angioplasty for monitoring purposes, due to cumbersome methodology and difficulty in approaching the patient (ultrasound scanner) and the need for contrast agent injections (ventricular angiography).

During angioplasty a thin wire which is threaded past the stenosis to the distal portion of the treated vessel is routinely used to guide a balloon (or other device for opening a blocked artery) to the stenotic site (Fig. 1). Since the guide wire (GW) is radio-opaque, and since it moves with the epicardial coronary arteries, information regarding myocardial function can be potentially extracted from the GW motion. Of particular interest is the ability to measure ventricular twist using this approach. The left anterior descending artery (LAD) segment curves around the apex, this segment being perpendicular to the long axis of the left ventricle (LV). Therefore, apex rotation can be easily measured by the angular motion of the apical wire segment as viewed from the septal view [6]. Although the information extracted from the GW is limited, i.e., it represents the motion of a single line on the epicardium, it is believed that even this limited data can teach us about some aspects of myocardial function during angioplasty [6], [16], [17]. When observing the GW motion throughout the angioplasty procedure, one can see changes in its movement pattern. In order to study these changes and clinically apply them during angioplasty procedures, an objective index must be obtained from this altered motion pattern. It is believed that this work is a step toward establishing such an index. It is clear that three-dimensional (3-D) information is lost by this method, but even the partial information acquired may give us important information regarding myocardial function and its changes during angioplasty. The dynamics of an extracted index with time may even contain further important information on the evolution of events throughout the cardiac cycle. The GW approach for analyzing myocardial motion offers a few advantages over prior techniques [11]. It resides in the coronary arteries during angioplasty and there is no need for additional equipment or injection of contrast agents. As discussed above, recent studies of apical twist [16], [17], point out the potential applicability of studying the apical twist from a single line. Altogether, the motion of the GW can provide an immediate practical tool for on-line beat to beat analysis of epicardial motion of the involved region, reflecting at least some aspects of the local myocardial function during angioplasty.

Manuscript received May 12, 1995; revised August 21, 1996. *Asterisk indicates corresponding author.*

D. Palti-Wasserman is with the Department of Biomedical Engineering, and the Faculty of Computer Science, Julius Silver Institute, Technion–Israel Institute of Technology (IIT), Haifa 32000 Israel.

A. M. Brukstein is with the Department of Biomedical Engineering, and the Faculty of Computer Science, Julius Silver Institute, Technion–Israel Institute of Technology (IIT), Haifa 32000 Israel.

*R. P. Beyar is with the Department of Biomedical Engineering, and the Faculty of Computer Science, Julius Silver Institute, Technion–Israel Institute of Technology (IIT), Haifa 32000 Israel (e-mail: rafael@biomed.technion.ac.il).

Publisher Item Identifier S 0018-9294(97)00294-2.

ANGIOPLASTY IN THE LAD RAO VIEW

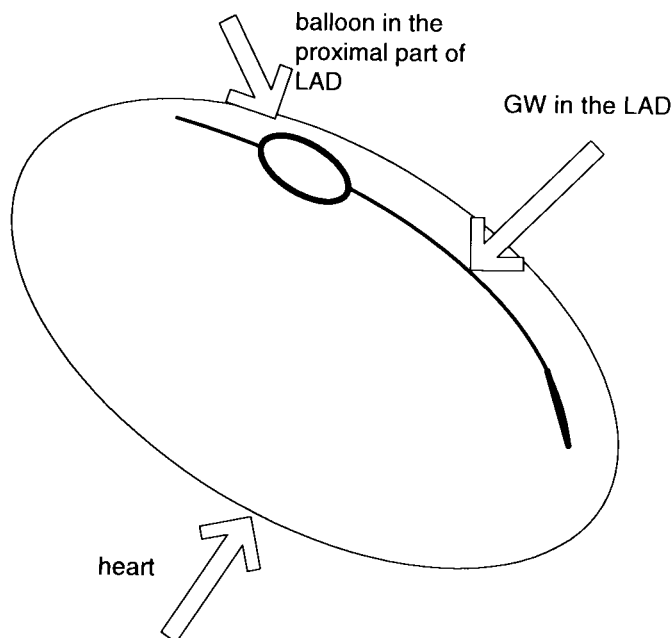


Fig. 1. A schematic illustration of the GW in the LAD artery, right anterior oblique (RAO) view. The wire is advanced to the distal portion of the LAD artery while the balloon inflation accrues at the proximal part of the artery.

The aim of this work is to provide tools for the detection and tracking of the GW using X-ray pictures taken during angioplasty. Since these pictures are of low quality—low contrast and low signal-to-noise ratio (SNR)—and since high reliability and high level of automation is required, none of the available methods in computer vision satisfy all these requirements [9], [11], [25]–[28], [31], [35]. There is a need for a new algorithm to be developed which will utilize the special characteristics of the GW in order to automatically extract it from the image.

The algorithm developed is based on working in limited active windows. It comprises two stages: the preprocessing stage and the tracking stage. The window preprocessing is aimed at the difficult task of enhancing the GW while suppressing the noise. Since low-pass filters tend to suppress both noise and the GW, while high-pass filters enhance both, two special filters were developed for the present algorithm. One is based on a Laplacian filter, while the other on a Marr–Hildreth filter [31]. After the preprocessing stage, the image was improved; however, the noise was still significant, resulting in a noncontinuous GW. To overcome this problem, the GW's tracking was based on fitting a second-degree polynomial, using the Hough transform [4], [10] to a part of the GW in a specific active window. To further

improve the results, numerous modifications of the basic algorithm were made, including an automatic tracking correction mode.

A single set of parameters, which enabled good tracking for a large number of images taken during angioplasty, was fitted to the final algorithm. The output of the algorithm was a set of points which describe the location of the GW.

II. METHODS

A. Data Acquisition

During angioplasty, relevant parts of the procedure are recorded on film. For the present work images of the heart with the GW in the LAD were obtained before, during, and after the inflation of the balloon in the proximal part of the LAD coronary artery. The wire was advanced to the very distal portion of the artery while balloon inflation occurs at the proximal part of the artery (Fig. 1). The images were projected off line on a screen and sampled to the memory of a PC computer with a CCD video camera (Grundig-Television Camera F/A 85I) and a frame grabber (PC Vision Plus, Imaging Technology Inc., Woburn, MA). The images were sampled with a resolution of 512×512 pixels and 8 b per pixel. The data was stored as bit-map-raw-data. The algorithm was performed on the above data.

B. Image Processing

1) *The Preprocessing Stage:* The X-ray images of the heart are characterized by low contrast, low SNR, uneven distribution of the noise in the image itself, and a change in the noise distribution in time sequence images. The signal that is to be extracted from the image is the GW which resides in the coronary arteries. Since the GW is only partially opaque to X-ray, and in addition it is only 0.0014-in. wide, it is of low contrast compared to the background. Furthermore, because of the low SNR the wire does not form a continuous image (Fig. 2). Thus, in order to track the wire under these conditions it is necessary to enhance the image of the wire before attempting to track it. The preprocessing stage is designed to enhance the GW while suppressing the noise. Since low-pass filters tend to suppress both noise and the GW, while high-pass filters enhance both, two special filters were developed.

The first filter is based on the classical Laplacian filter

$$\begin{bmatrix} 1 & 1 & 1 \\ 1 & -8 & 1 \\ 1 & 1 & 1 \end{bmatrix} \quad (1)$$

It uses global information in an attempt to enhance the GW in the image without enhancing the noise. Each point in the image is compared not to its closest neighbors, i.e., to the points surrounding it, (as done in the usual 3×3 Laplacian filter), but rather to more distant points in the image. The

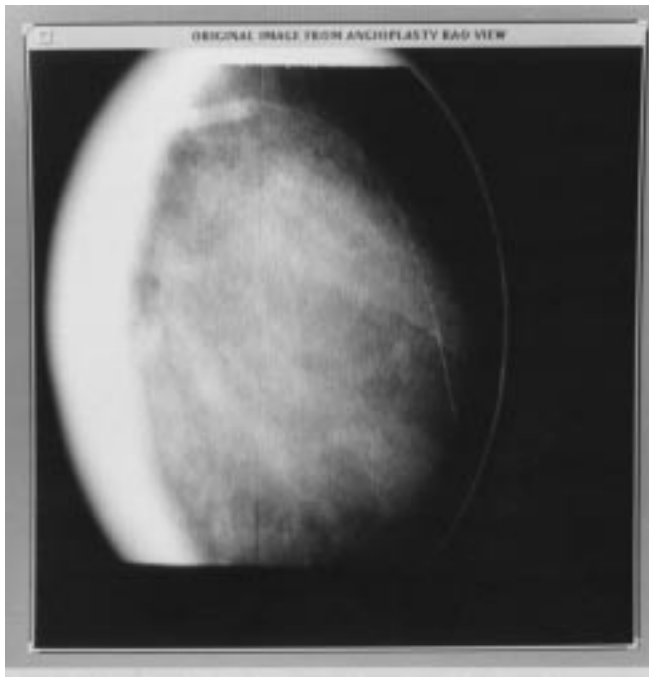


Fig. 2. An X-ray image of the GW in the heart during percutaneous transluminal coronary angioplasty (PTCA) in RAO view. The image is characterized by low contrast, low SNR, and uneven distribution of the noise. This results in a noncontinuous image of the GW.

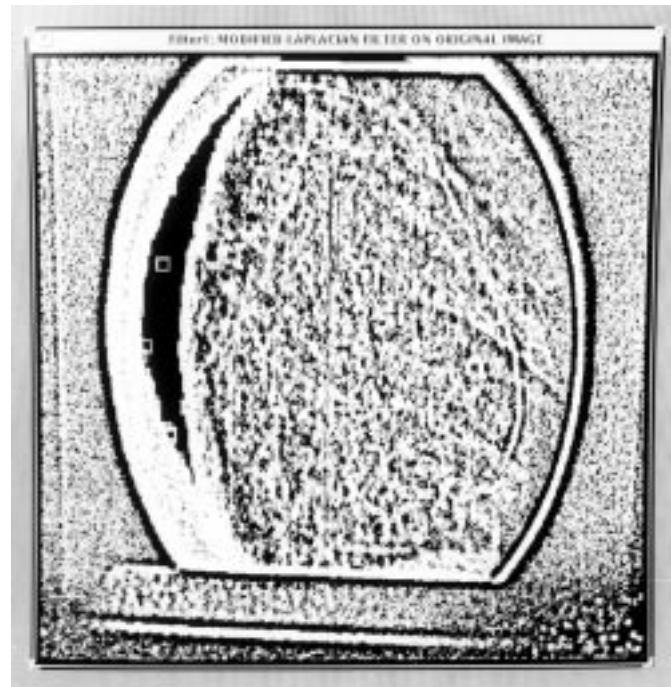


Fig. 3. The image in Fig. 2 processed by modified Laplacian filter. The filter suppresses local noise and enhances global changes in the image. Thus, it succeeded in enhancing the GW and suppressing the background noise. Although filtered the GW image is still noncontinuous.

modified Laplacian filter used here is given by

$$\begin{matrix}
 1 & 1 & 1 & 1 & 1 & 1 & 1 & 1 & 1 & 1 & 1 \\
 1 & 0 & 0 & 0 & 0 & 0 & 0 & 0 & 0 & 0 & 1 \\
 1 & 0 & 0 & 0 & 0 & 0 & 0 & 0 & 0 & 0 & 1 \\
 1 & 0 & 0 & 0 & 0 & 0 & 0 & 0 & 0 & 0 & 1 \\
 1 & 0 & 0 & 0 & 0 & 0 & 0 & 0 & 0 & 0 & 1 \\
 1 & 0 & 0 & 0 & 0 & 0 & 0 & 0 & 0 & 0 & 1 \\
 1 & 0 & 0 & 0 & 0 & -40 & 0 & 0 & 0 & 0 & 1 \\
 1 & 0 & 0 & 0 & 0 & 0 & 0 & 0 & 0 & 0 & 1 \\
 1 & 0 & 0 & 0 & 0 & 0 & 0 & 0 & 0 & 0 & 1 \\
 1 & 0 & 0 & 0 & 0 & 0 & 0 & 0 & 0 & 0 & 1 \\
 1 & 0 & 0 & 0 & 0 & 0 & 0 & 0 & 0 & 0 & 1 \\
 1 & 0 & 0 & 0 & 0 & 0 & 0 & 0 & 0 & 0 & 1 \\
 1 & 0 & 0 & 0 & 0 & 0 & 0 & 0 & 0 & 0 & 1 \\
 1 & 0 & 0 & 0 & 0 & 0 & 0 & 0 & 0 & 0 & 1 \\
 1 & 1 & 1 & 1 & 1 & 1 & 1 & 1 & 1 & 1 & 1
 \end{matrix} \tag{2}$$

This filter suppresses local noise and enhances the global changes in the image (Fig. 3). The size of the filter and its actual structure take in to account the width of the GW and the characteristics of the noise. The best results for using this filter were obtained by using a 11×11 filter. Each point is compared to all the points which are five pixels distant from it. Instead of using ordinary zero crossing, as is usually done with Laplacian filters, a threshold which was not zero was chosen. One advantage of using the modified Laplacian filter described is that the filter consists mostly of zeros, making the filtering stage fast compared to other filters which give similar effects on the image.

The idea is to smooth the Laplacian filter in order to try to further suppress the background noise. The result is a filter which resembles the Marr–Hildreth filter [31] and has the

shape of a Mexican hat

$$\begin{matrix}
 3 & 3 & 3 & 3 & 3 & 3 & 3 & 3 & 3 & 3 & 3 \\
 3 & 7 & 7 & 7 & 7 & 7 & 7 & 7 & 7 & 7 & 3 \\
 3 & 7 & 1 & 1 & 1 & 1 & 1 & 1 & 1 & 7 & 3 \\
 3 & 7 & 1 & -3 & -3 & -3 & -3 & -3 & 1 & 7 & 3 \\
 3 & 7 & 1 & -3 & -20 & -20 & -20 & -3 & 1 & 7 & 3 \\
 3 & 7 & 1 & -3 & -20 & -148 & -20 & -3 & 1 & 7 & 3 \\
 3 & 7 & 1 & -3 & -20 & -20 & -20 & -3 & 1 & 7 & 3 \\
 3 & 7 & 1 & -3 & -3 & -3 & -3 & -3 & 1 & 7 & 3 \\
 3 & 7 & 1 & 1 & 1 & 1 & 1 & 1 & 1 & 7 & 3 \\
 3 & 7 & 7 & 7 & 7 & 7 & 7 & 7 & 7 & 7 & 3 \\
 3 & 3 & 3 & 3 & 3 & 3 & 3 & 3 & 3 & 3 & 3
 \end{matrix} \tag{3}$$

The size of the filter, and the degree of smoothing are important parameters of this filter. Another parameter which can be altered to improve results of this filter is changing the threshold used for the zero-crossing from zero to a different threshold value; thus applying a “pseudo” zero-crossing procedure. This filter, the modified Marr–Hildreth filter, gave better results than the first filter (the modified Laplacian filter), but it requires more calculation time (Figs. 3 and 4).

After using one of the above filters, convolving the image with the filter and finding the “pseudo” zero-crossings, the image is transformed to a binary image, the “pseudo” zero-crossings are turned into white, and the rest of the image is turned into black. This binary image is used as an input image to the next stage of the algorithm, which is tracking the GW from the improved filtered image (Figs. 3 and 4).

2) *Basic Guided Wire Tracking Procedure:* The output of the preprocessing first stage is a binary image with reduced noise and an enhanced wire. The problem is that the image

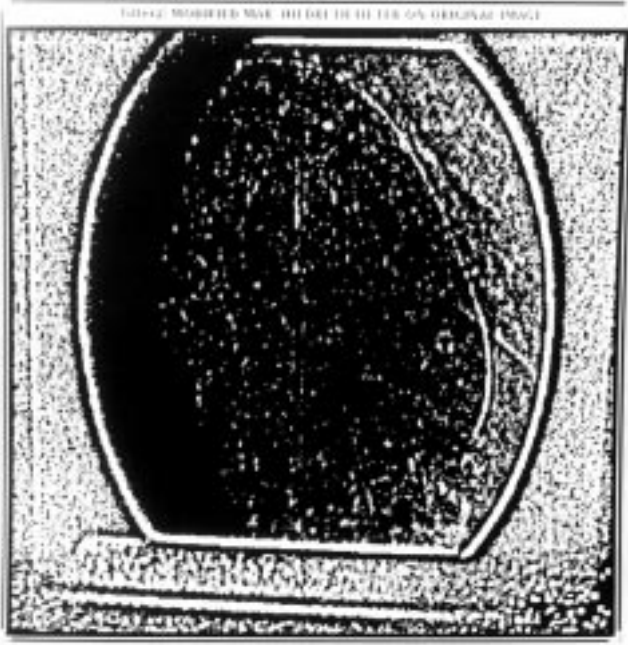


Fig. 4. The image in Fig. 2 processed by the modified Marr–Hildreth filter. The filter suppresses local noise and enhances global changes in the image. Thus, it succeeded in enhancing the GW and suppressing the background noise. Although filtered the GW image is still noncontinuous.

of the wire appears as a noncontinuous white image on a noisy spotted background (Figs. 3 and 4). Another problem which makes tracking the wire difficult is the fact that the wire is flexible and therefore changes its shape as well as its location with time.

The tracking algorithm was developed to overcome these problems. The tracking is based on fitting a second-degree polynomial to the GW, while using local and global information from the image, including *a priori* information about the characteristics of the GW.

The shape of the GW suggests fitting it with a second-degree polynomial. To do so, the Hough transform for curve fitting is used [4], [10], [22]. A second-degree polynomial is defined by three parameters a , b , and c as follows:

$$y = ax^2 + bx + c. \quad (4)$$

To calculate the values of these three parameters for the polynomial, one needs to know three points which belong to this curve. If we assume that we know two points that belong to it, this means that the curve can be represented by only a single parameter, thus reducing the complexity of the representation from three parameters to one parameter. Therefore, by assuming that the locations of two points on the GW are known, it is possible to simplify and represent the GW with a second-degree polynomial with a single parameter. The parameter which was chosen to represent the GW in the present algorithm was b . Thus now, when representing the GW with a second-degree polynomial, every point on the GW can be represented by a single parameter, in this case the parameter b .

In order to use the Hough transform for curve fitting on the image, the value of b for every white point in the image was

calculated, under the assumption that two points on the GW are already known (see Appendix A). The Hough transform is then applied to the image with the calculated b values. This means that a special vector is used to count the number of appearances of each value of b in the image. This vector will be referred to as b -count and in practice, it is the b histogram of the image. As in all Hough transforms, the b parameter, with the largest number of counts represents the polynomial which passes through the largest number of white points in the image. After choosing the b parameter the two other parameters, a and c , can be calculated as well (Appendix A), thereby fitting a second-degree polynomial to the GW.

3) *Working in Overlapping but Limited Active Windows:* Since the entire length of the GW cannot be described by a single second-degree polynomial, it must be represented by a series of second-degree curves. To do so, the image is then divided into overlapping smaller areas, called limited “active windows.” A second-degree polynomial is fitted to the part of the GW passing through each window.

By applying the preprocessing and tracking algorithm in limited active windows, many advantages are gained. In each window, the preprocessing is activated and a second-degree polynomial is fitted by using the Hough transform to part of the GW in the specific window. Using the preprocessing in limited areas decreases the preprocessing computation time. Using the polynomial fitting on overlapping limited windows enables us to rely on characteristics of the GW such as continuity and smoothness. Thus, local and global information are being used simultaneously. Note that the size of the active window increases, the amount of noise points grows proportional to the area, while the number of points belonging to the GW increases linearly; therefore the SNR decreases. On the other hand, as the size of the subarea decreases it contains less information and, especially, less global information on the GW. Therefore, the size of the window is an important parameter and must be carefully chosen.

The actual tracking is done in the following manner.

a) *First tracking procedure:*

- After the original image is acquired, two points on the GW near its end are located and entered manually (X_0, Y_0) (X_1, Y_1) .
- An active window with (X_1, Y_1) as center is defined. This becomes the present working area. The size of the active window which gave the best results (sufficient information on the GW, some global information, and improved SNR) was found by trial and error to be 71×71 pixels.
- The above defined window is preprocessed and a binary subimage is produced.
- The binary subimage is then sent to a second routine which fits the second-degree polynomial by using the Hough transform, as explained previously. The output of this routine is a set of three parameters, representing the fitted polynomial in the present active window.
- Using the selected polynomial’s parameters $(a, b, \text{ and } c)$ and the center point of the present active window (X_1, Y_1) , the point (X_2, Y_2) at which

THE BASIC TRACKING PROCEDURE

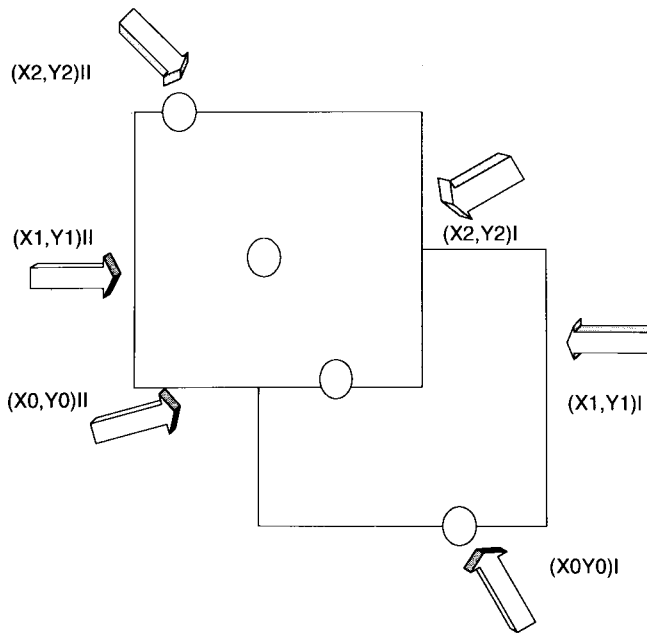


Fig. 5. A schematic illustration of the basic guided wire tracking procedure. The illustration demonstrates the use of the overlapping but limited active windows for tracking the GW image.

the polynomial leaves the present active window is determined.

b) Second tracking procedure:

- Two new points must be calculated to serve as initial points to start the algorithm again. Since consecutive windows overlap, two known points from the previous window can be used as initial conditions for the next window.

The center point (X_1, Y_1) from the present tracking stage is going to be the first initial point of the next window, and the point (X_2, Y_2) from the present window will be the second initial point for the next active window. This is described as follows:

$$\begin{aligned} (X_1, Y_1)^i &\Rightarrow (X_0, Y_0)^{i+1} \\ (X_2, Y_2)^i &\Rightarrow (X_1, Y_1)^{i+1} \end{aligned} \quad (5)$$

i , being the number of tracking stage, i.e., the label of the active window.

Thus, the above tracking procedure (Fig. 5), when given only two initial points, insures that each active window automatically receives its own two initial points. Furthermore, tracking in the described manner results in a 50% overlap of the windows, which provides continuity and smoothness of the tracking curve [Fig. 6(a) and (b)].

c) *Further improvements of the tracking procedure:* The above described basic tracking algorithm did not give suffi-



(a)



(b)

Fig. 6. The steps in tracking the GW in an X-ray image using overlapping but limited active windows. (a) First step in tracking the GW. (b) Second step in tracking the GW.

ciently good results, when used on different images. Further improvements that were used are detailed below.

4) *Tracking Resolution Problems:* A constant resolution is essential for using the same constants for all active windows. Since a different range of b values is obtained in each window, in order to maintain a constant resolution of b in all windows, the length of the vector b_count must be allowed to vary so as to ensure that the resulting b vector resolution will be constant in each window. The length of the vector is determined in

such a way that the resolution of the b vector will be constant in each window

$$\text{Vector length} = (B_{\max} - B_{\min}) * \text{Resolution Constant.} \quad (6)$$

A good resolution for the b vector must also be selected. Using high resolution results in good precision in the value of the selected b , but results in a problem in detecting the peak of the b histogram, since a very flat b histogram is typically obtained. This difficulty in determining the histogram peak causes a problem in selecting the b , which represents the “best” polynomial which passes through a maximal number of white points in the image. On the other hand, if we work with low resolution, a peak in the b histogram is easy to detect, but the price we pay is that the selected b value is not accurate enough. The resolution chosen must be such that changes of one unit in b are not significant in the fitting results, but must also yield a significant peak in the b histogram. But no value for the b resolution could fulfill these requirements and thus give good tracking results.

The proposed solution is the simultaneous use of high and low resolutions. This is done by working with a very high resolution for the b 's, but simultaneously updating neighbors in the b vector in order to generate a peak in the b histogram. This solution gives the desired result of combined high precision and detectable peaks. For updating neighbors, in this manner, a filter in the b “plane” (a one-dimensional plane) called “*add_zone*” was used. The effect of this filter is that each time the counter of a specific b is to be updated, the filter also updates the counts of its neighboring b 's as well. The optimal length of the *add_zone* filter had to be found experimentally. A “long” filter will cause an accumulation of counts, thus creating peaks. However, using a filter which is “too long” will act as a Low Pass Filter, thus blurring the histogram peaks. To find the optimal length for the *add_zone* filter, a b histogram was calculated for different filter lengths. In addition, 3-D graphs of the b -count as a function of b and the filter length were used (Fig. 7). The filter length was chosen with the help of these graphs to be ± 200 . This filter helped forming peaks in the b histogram and, at the same time, it improved the algorithm's sensitivity to an error in the initial selection of points.

5) *Using Special Properties of the Guide Wire*: Some properties of the GW and the X-ray images have already been considered in the algorithm. The continuity and smoothness of the wire were already used in the algorithm. For example, in the preprocessing stage a filter was developed adapted to the specific GW image. Even more, in the basic tracking algorithm, the use of the Hough transform and the overlapping of the active windows also makes use of smoothness and continuity of the GW. In order to further improve the tracking process, additional information concerning the GW's characteristics must be added.

- a) In order to use the *a priori* information concerning the wire width, an additional filter was used. The idea was to give an advantage to tracking white point ensembles, rather than fitting random white points. Thus the tracking procedure will not be drawn toward any white point in

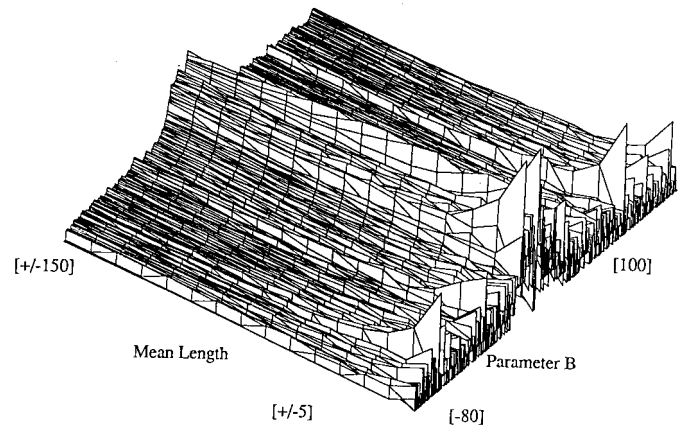


Fig. 7. The b Histogram as a function of the *add_zone* filter length. The Histogram is used to choose the optimal length of the *add_zone* filter. It can be seen that a long filter will create peaks but using a filter which is “too long” will smooth the histogram peaks.

the image, rather it will be drawn especially to white point ensembles, i.e., continuous lines with some width. As a result, random white points will have a smaller effect on the tracking. This will decrease the chances of failure of the algorithm due to tracking random noise. A two-dimensional Gaussian filter in the image plane was used to apply this idea to the algorithm.

Since the average width of the GW is three pixels, a three by three filter called *filter_cloud* was introduced. It was defined as

$$\text{FILTER-CLOUD} = \begin{matrix} 1 & 2 & 1 \\ 2 & 4 & 2 \\ 1 & 2 & 1 \end{matrix} \quad (7)$$

This filter *filter_cloud* is used to enhance the effect of white points which have white neighbors in the image plane. The idea is that the b count of a certain point will increase by more, if its neighbors are white points. If all its neighbors are white, than its count will increase by 16. If all its neighbors are black its count will increase only by four.

- b) Since we are tracking a physical wire which resides in the coronaries, the value of b representing the polynomial estimation of the GW cannot receive any value. There are limitations to the value the b parameter can receive. Very high values or very low values of b are not physical, since they correspond to polynomials that cannot represent the GW in the LAD from the RAO view. Thus the b values were limited as follows:

$$\text{if } -10^{10} > b \vee b > +10^{10} \implies \text{omit } b. \quad (8)$$

- c) Since the wire resides in the coronary arteries, its shape characteristics are closely linked with those of the arteries, thus the angles of the wire are also quite limited. Since the arteries do not change their angles abruptly, the wire residing in them can not have sudden angle changes (this induces some limitations on second derivatives). When looking specifically at the LAD it is also evident

that the shape of the LAD usually remains “convex” along its entire length in the RAO view, i.e., no inflexion points are seen. Therefore, b values which represent polynomials which do not presume this property, can again be omitted. To identify the b values which do not represent this property, i.e., convexity, a parameter called $b_straight_line$ is calculated for each active window. This parameter represents the b value of the polynomial, where $a = 0$, i.e., a straight line which passes through the two initial points. This parameter is used to limit the chosen b values, i.e., limits the legal polynomials, only to those which are “convex” ones. For polynomials which are represented as a function of $x: y = f(x)$, the limitation will be as follows:

$$\text{if } b < b \text{ straight line} \implies b \text{ is not convex} - \text{omit } b. \quad (9)$$

This limitation is very rigid and it does not permit the tracking algorithm to correct its own minor mistakes, since the tracking must be always convex. In an attempt to avoid this problem, a degree of freedom is given to the tracking polynomial. It has to be convex, or almost convex. This is done by using a less harsh criterion for omitting the illegal b 's, i.e., allowing a small amount of deviation from a straight line

$$\text{if } b < b \text{ straight line} + \delta \implies \text{omit } b. \quad (10)$$

6) *Considering the Main Direction of the Wire:* In order to estimate the GW in the best possible way, it is necessary to use as many points as possible inside the active window. Therefore, great significance should be assigned to the GW direction inside a specific window. The direction of the GW is determined by the position of the entering point of the GW into the active window (right or bottom). If the GW enters from the bottom of the window, it is best described by a function of $x: y = f(x)$. If the GW enters from the right side of the window, it is best described by a function of $y: x = f(y)$. Accordingly, the best representation of the polynomial is chosen for the algorithm for each active window. The algorithm then splits to one of two symmetrical cases. For each case the parameters and constants are calculated a little differently.

7) *Considering the b Histogram in an Active Window:*

a) From a study of the b histogram in different windows, it is apparent that the high counts in the b histogram are concentrated over a narrow region. Therefore, it is not necessary to search the entire b span for obtaining the maximum of the b histogram. Searching only over a narrow region is sufficient. This information is incorporated into the algorithm.

An initial b vector is searched for a region where the counts are above a predetermined threshold. Only this region is used for the next stage. In the next search, a new b vector with a higher resolution which includes only the above selected region is used. The final b is chosen from this high resolution b vector.

b) The b histogram in an active window is characterized by ensembles of close peaks for each local maximum region in the histogram. We are interested in retaining several different optional b values for tracking, so if a wrong curve is chosen at some point, the error can be corrected by backtracking and using yet another peak. Since high resolution in the b vector is used, this results in quite close values for the selected b 's. Therefore, it is necessary to alter the search for the maximas in the b histogram, to avoid this phenomena, i.e., find several different peaks. This is done before searching for the peaks in the b histogram, by a reduction of the original b histogram, to avoid redundant information. From every N successive b values in the original b histogram, only the one with the largest number of counts is left and transferred to the reduced histogram, which is used for the maxima search. It should be noted that using a large N can result in too dramatic reduction, which may cause loss of essential peaks in the histogram.

8) *Manipulating the Picture Coordinates:* From the analysis of the sensitivity functions of the tracking parameter b as a function of the spatial coordinates, it is apparent that there is a high dependency of the parameter b on the specific spatial coordinates which is described by the following equations:

$$y = ax^2 + bx + c \quad (11)$$

$$b(x, y) = \frac{y}{x} - ax - \frac{c}{x} \quad (12)$$

$$\frac{db}{dx}(x, y) = -a + \frac{c-y}{x^2} \quad (13)$$

$$\frac{db}{dy}(x, y) = -\frac{1}{x}. \quad (14)$$

This dependency is generally undesirable. It does not permit using the same parameters and constants (such as resolution for example) on different windows. In other words, parameters that work well with in a window whose origin is (0, 0) do not necessarily work well with a window whose origin is (70, 70). The parameters of the algorithm and constants must be independent of the coordinates of the active window. The desired sensitivity function should be as constant as possible. By looking at the above equations it is obvious that when X and Y have high values, the sensitivity function is almost constant, which is the desired effect.

Thus, to overcome the undesired effect of coordinate dependency, the image of each active window is transferred to a new set of coordinates with very high values. By transferring each active window to coordinates (10 000, 10 000) for example, we obtain a tracking algorithm with almost no sensitivity to the coordinates within the window and between windows. The algorithm is thus made invariant to the specific windows coordinates.

9) *An Error Correcting Option for the Tracking Procedure:* High reliability standards are required from this algorithm. Even when using all the disclosed improvements in the identification and tracking of the GW, the algorithm is not sufficiently error free. Further improvement is needed. To further decrease the number of tracking errors, an error correcting procedure was added to the algorithm.

To apply an error correcting procedure the first step was to define a criteria for tracking quality, and the second step was to define when a tracking step has failed. Two such criterions were defined: 1) If none of the calculated b values which have high counts are legal (this means that the b values are very high or they represent nonconvex polynomials)—the tracking is not valid. 2) If the count value in the present active window is less than 50% than the count of the previous active window—the tracking is not valid. Once such problems are detected in a certain active window a correction procedure is activated.

The correction is exercised in the following way. The center point of the current active window (X_1, Y_1) is moved from its original position to the left and to the right in single pixel steps (± 4 pixels). Altogether, eight new positions. For each of these new positions of (X_1, Y_1) the fitting of the polynomial, i.e., calculating the b_count vector and finding its maxima, is repeated. From the eight b values (which represent the b values with the maximum counts for each position), the b with the higher count is selected as the b representing the polynomial best fit for the present window. This procedure was experimentally found to significantly improve the number of successful tracking.

III. RESULTS

A. Simulation

In order to test the performance of the tracking algorithm, a simulation image was used. The tracking algorithm without the tracking error correction procedure was applied to an artificial simulated image. The advantage of applying the algorithm on a simulated image is that the exact location of the GW is known, and the amount and characteristics of the noise are also a known variable. With the aid of the simulated image, the success of the algorithm was tested, as well as the influence of different algorithm parameters on the quality of the tracking. The parameters tested for their influence on the success of the algorithm were: size of active window, amount of coordinate shift, resolution of the b vector, the lengths of the filters, and more.

Using the simulation, optimal values were selected for the different parameters used in the algorithm. A set of optimal parameters is defined as a single set which gives good tracking results in as many different images as possible.

1) *Creating the Simulation Image:* The simulated image is composed from a white curve on a black background with noise added as random white points. The curve is a second-degree polynomial. The random noise is of uniform distribution upon the whole image (Fig. 8). Two types of simulation images (512×512 pixel image consisting of 256 000 points), were used. The first image type had a low level of noise (20 000 points per image), and the second had a higher level of noise (125 000 points per image).

2) *Tracking the Wire in a Simulated Image:* The tracking algorithm (without the tracking correction option) was used on the two types of simulated images described above. The

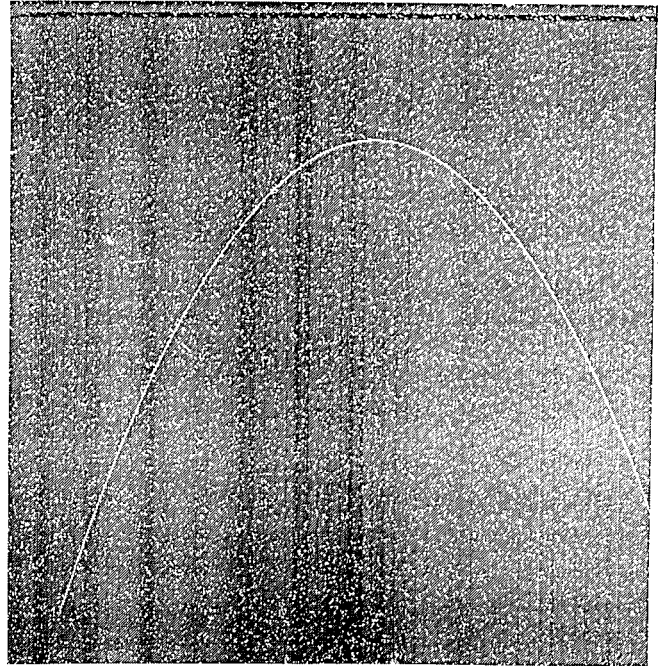


Fig. 8. The simulated image comprising of a white curve on a black background and 256 000 random white points which were added to the image as noise.

algorithm was applied many times, each time on a different simulated image, either on the low noise level image or on a high noise level image. In order to check the behavior of the tracking as a function of the parameters, the parameters of the algorithm were changed between runs. For example, the simulation was run with and without coordinate shift in the image and then, it was run with different values of coordinate shift. Thus, an optimal shift value which gives good tracking along the GW was found for each of the noise levels. Other parameters were varied as well. The resolution of the b vector was altered between 0.02–1. The length of the filter add_zone was changed between 30–500. The amount of reduction in the b vector was altered between zero reduction ($N = 0$), and a large reduction ($N = 50$). The initial resolution of the b vector was changed between 100–10 000.

From these simulations, an optimal set of parameters was chosen (the parameters which gave good tracking for as many simulated images as possible). The sensitivity of the algorithm to the initial starting point was checked, using the optimal set of parameters. The initial starting points, are the two points entered manually by the user at the beginning of the tracking algorithm. By altering these points, and checking if the tracking algorithm succeeds in tracking even when these points are entered inaccurately, the sensitivity to the starting points can be checked.

3) *Simulation Results:* A few sets of parameters that gave good tracking for many simulated images were found. An example of such a set is detailed in Table I. A dependency between the level of noise and some of the parameters was found. For example, the amount of coordinate shift needed depended on the amount of noise in the image. The sensitivity

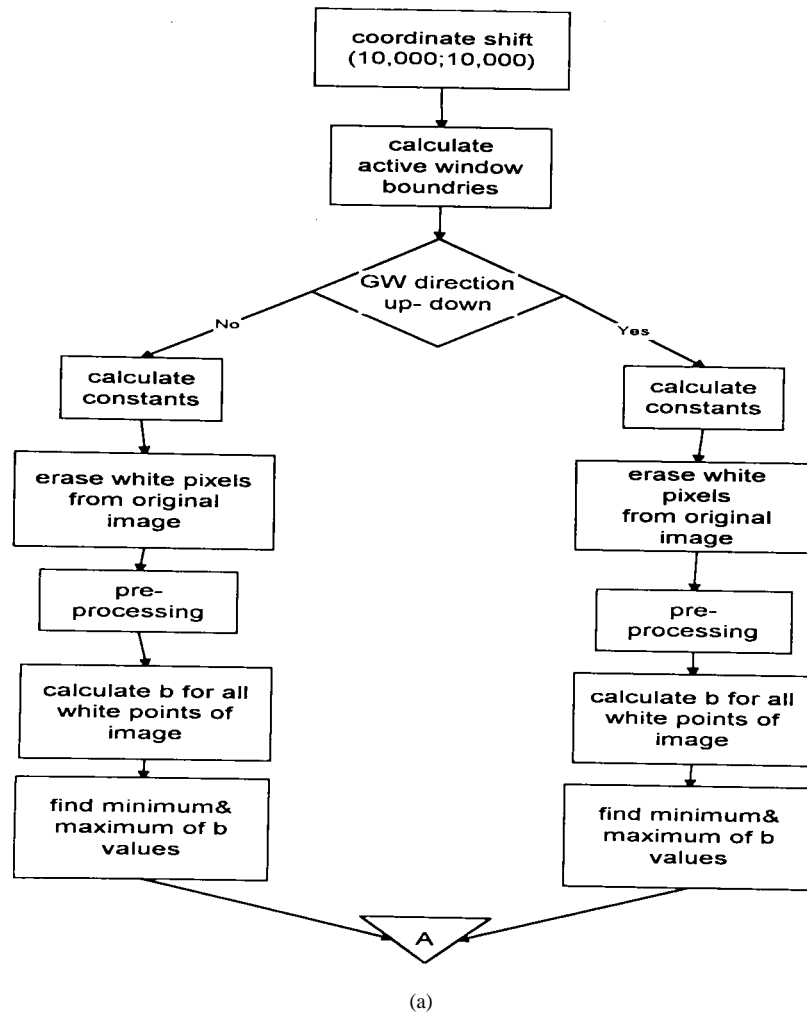


Fig. 9. (a) A flow chart of the final tracking algorithm for angioplasty images.

of the algorithm to the input of inaccurate initial points was low. In most of these cases the algorithm managed to correct itself and continue the tracking in an accurate manner.

B. Using the Algorithm on Realistic Images Obtained During Angioplasty

The results and conclusions from using the algorithm on the simulated image were studied and applied to the images from angioplasty. A flow chart summarizing the final tracking algorithm is presented in Fig. 9(a)–(c). Since a dependency between the different parameters and the noise level was found, the optimal parameters found for the simulated image had to be altered in order to fit the angioplasty images which had a different noise level.

The noise level of the angioplasty image was close to the simulated image with the high level of noise. Therefore, the parameters found for the high noise level simulation were used as initial parameters for the algorithm when used on angioplasty images. These initial parameters were altered until an optimal set of parameters that gave good tracking results for a large number of different angioplasty images (see Table I).

Using the above set of parameters the final algorithm including the error correcting procedure was applied to 31 different images acquired during angioplasty. The images used included images recorded before, during, and after the balloon inflation. Good tracking along the wire was accomplished in all 31/31 images (Fig. 10).

To check the sensitivity of the algorithm to its starting points, the algorithm was run on different images with the starting points intentionally moved away from the GW. In 16 of the 31 images, the tracking was successful when the starting points were moved. Thus, the sensitivity of the algorithm to its starting points is low.

IV. DISCUSSION AND CONCLUSIONS

Transient coronary occlusion during angioplasty causes abnormal function in the region supplied by the treated vessel due to transient ischemia [12], [20], [21]. It is, therefore, of clinical importance to be able to monitor the degree of abnormal function and its return to baseline during and between multiple balloon inflations of variable durations. In order to monitor beat-to-beat motion of the myocardium there is a need to

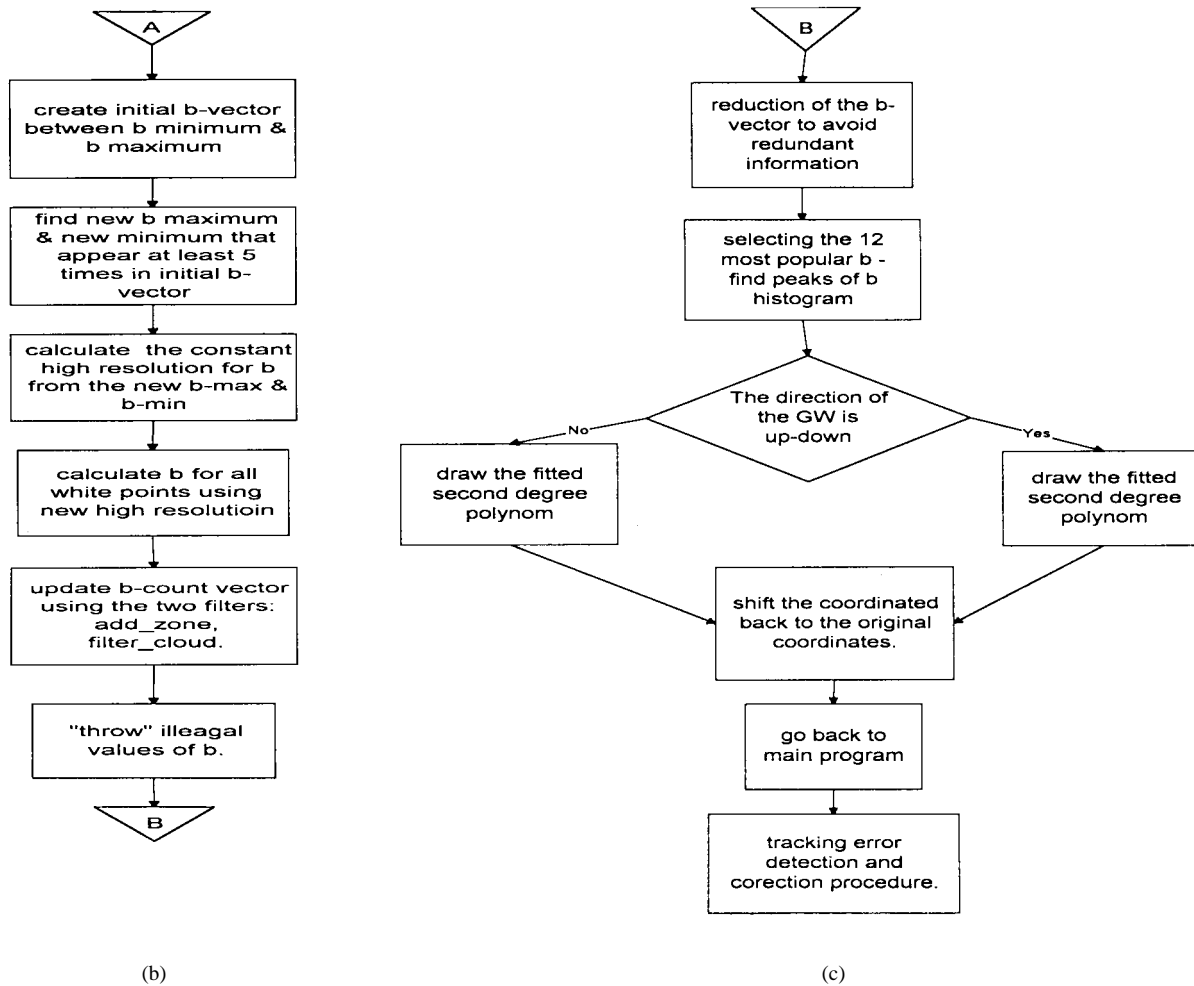


Fig. 9. (Continued.) (b), (c) A flow chart of the final tracking algorithm for angioplasty images.

reduce the amount of data representing myocardial motion. Thus, an objective automatic set of indexes must be used to represent myocardial function.

Since the GW resides in the coronary arteries and the arteries move with the epicardium, it is believed that information regarding the mechanical function of the myocardium can be extracted from the movement of the GW. This information does not represent the full scope of myocardial function, but can provide partial vital information regarding myocardial function. Abnormal function of the myocardium is believed to be easily detectable in the movement of the GW, even when observing its motion by visual eye inspection. Thus the GW can provide valuable information regarding myocardial function. Furthermore, by monitoring the changes in the GW it could be possible to guide the time period between balloon inflations in correlation with the muscle recovery rate.

The GW can give the option of monitoring either central motion of the myocardium from the radial view for a GW in the LAD or nonradial motion such as twist [37]. In both motion types, changes in the GW motion are visually noticeable. Recent work on apical twist [16], [17] emphasize the potential of the apical rotation or twist that can be readily measured with the GW approach in reflecting myocardial function. More specifically, recent studies on apical twist [16], [17]

demonstrate that the information regarding apical twist can prove to be important both, in a clinical and pure research basis. Thus, since the method provided here can indeed support monitoring of nonradial motion such as apical twist, in addition to other applications, it has great potential in studying and monitoring apical motion. To conclude, the GW can provide on-line beat-to-beat dynamic information regarding regional or global ventricular function without exposing the patient to additional risks.

To date, only very limited studies have been conducted, which monitor myocardium function and recovery during percutaneous transluminal coronary angioplasty (PTCA). Some of the studies used echocardiography, while others used X-ray-based ventriculography [5], [29], [34]. These studies were done on limited groups of people that usually included patients with only one stenosis and no preliminary dysfunction in heart muscle. The analysis done in these studies was off-line and slow since nonautomatic procedures were used. Thus these methods cannot provide us with a clinical tool for active monitoring of myocardial function.

This work is a step toward an algorithm that would automatically track and analyze the motion of the GW during PTCA, to enable real time monitoring of mechanical myocardial function.

TABLE I
THE FINAL (OPTIMAL) SET OF PARAMETERS USED IN
THE ALGORITHM FOR SIMULATED AND ANGIOPLASTY IMAGES

	Simulated	Final
Size of active window	61 x 61 pixels	71 x 71 pixels
Coordinate shift	(10,000 10,000) pixels	(10,000 10,000) pixels
Initial length of b vector	4000	4000
Threshold for using second resolution	5	5
Length of <i>add_zone</i> filter	± 200	± 200
Amount of b histogram reduction	10	30
Amount of curvature deviation from straight line	± 0.3	± 0.3
Number of histogram peaks selected	12	12
Constant high resolution	0.08	0.04

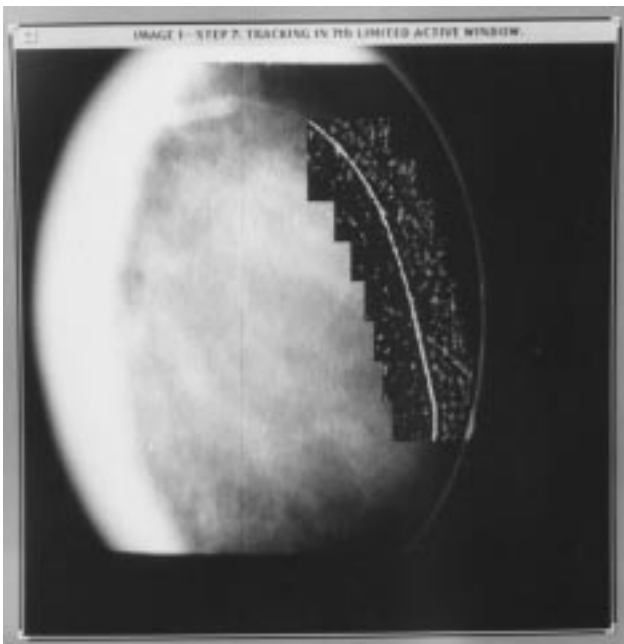


Fig. 10. Successful tracking of the GW in an X-ray image during PTCA. The tracking was done using the final tracking algorithm with the optimal set of parameters selected in this work for angioplasty images.

In this work, X-ray images of the heart were used during angioplasty. These images are typically of poor quality: low contrast, low SNR, and considerable variance between consecutive images in time. The GW that is to be extracted is only one to three pixels wide while the noise level is high. This results in an image of a noncontinuous GW.

The requirements from the algorithm are high level of reliability and some level of automation in order to form a foundation for a fast algorithm that requires minimum human involvement. Image processing algorithm developed previously and algorithms developed for tracking and identifying in medical images do not meet these requirements [9], [11], [25]–[28], [31], [35]. There is a need to write a unique algorithm which is dedicated specifically to the angioplasty images. This algorithm will include *a priori* information about the GW characteristic shape and some of the image characteristics. The algorithm discussed here uses *a priori* information and incorporate it in the algorithm.

The first stage of the algorithm is a preprocessing stage which is aimed at improving SNR by enhancing the GW while suppressing the noise. When using standard filters like low-pass filters that suppress noise, the GW itself, which is very narrow (one to three pixels), was suppressed along with the noise. Thus, the SNR was not improved. On the other hand high-pass filters which enhanced the GW, enhanced the noise as well; thus again no improvement in the SNR was gained. The standard filters did not succeed in improving the image, since the noise and the GW are of very similar characteristics. Other operations on the image, such as histogram stretching, histogram equalization with a combination of different filters used on either the whole image or on selected areas of the image, also did not improve the image.

The conclusion was that a special filter has to be developed specifically for X-ray images of the GW during angioplasty. Two such filters were developed for this purpose. One was a modified Laplacian filter, and the other was a modified Marr–Hildreth filter. The second filter gave better results, but requires more calculation time.

The second stage included tracking of the GW. The problems associated with the tracking stage are that even now, after the preprocessing, the SNR is still low—the GW is not continuous. This results in areas of the image where the GW does not seem to exist at all and other areas where the noise points look as part of the GW. Another difficulty in tracking the GW is caused by the fact that it does not move as a rigid object and changes its shape as well as its position. This is why it was necessary to use *a priori* information on the GW shape and position, and the characteristics of the noise. To incorporate all these in the tracking stage, global and local processes had to be used in the algorithm.

The tracking is based on fitting a second-degree polynomial in a limited active window. This has many advantages, among them that by overlapping the areas of these windows one can obtain continuity as well as smoothness of the tracking polynomial; thus global and local information are being used simultaneously. Many additional improvements were entered in to the algorithm. A simulation image helped focusing on the weak points of the algorithm and improving them. A single set of optimal parameters, which enabled good tracking for a large number of images taken during Angioplasty, was fitted to the final algorithm. With these parameters and the aid of an error correcting option for the tracking procedure, adequate results were obtained with 100% correct tracking on the 31 images tried.

This algorithm can be further developed in the future in several directions. In order to increase the automation, tracking of the GW in time must be added to the algorithm. More characteristics of the angiography image may be included in the algorithm to further improve its performance. In addition, the algorithm must be tested off-line on different images from angioplasty in order to try and characterize and analyze the changes in the GW motion resulting from balloon inflation and transient ischemia.

APPENDIX

CALCULATING b AS A FUNCTION OF (x, y) , WHEN THE INITIAL STARTING POINTS ARE KNOWN

A GW is represented by a second-degree polynomial

$$y = ax^2 + bx + c. \quad (A1)$$

The two known points that belong to the polynomial are

$$\begin{aligned} (x_0, y_0) \\ (x_1, y_1), \end{aligned} \quad (A2)$$

Therefore, we can write the following equation:

$$y_0 = ax_0^2 + bx_0 + c \quad (A3)$$

$$y_1 = ax_1^2 + bx_1 + c. \quad (A4)$$

Using these two equations we can write for a and c

$$a = \frac{(y_1 - y_0) - b(x_1 - x_0)}{x_1^2 - x_0^2} \quad (A5)$$

$$c = y_0 - ax_0^2 - bx_0 \Rightarrow$$

$$c = y_0 - x_0^2 \left(\frac{y_1 - y_0}{x_1^2 - x_0^2} \right) + x_0^2 \left(\frac{x_1 - x_0}{x_1^2 - x_0^2} \right) b - bx_0. \quad (A6)$$

So the second-degree polynomial can be written as follows:

$$\begin{aligned} y(x) = & \left(\frac{y_1 - y_0}{x_1^2 - x_0^2} \right) x^2 - b \left(\frac{x_1 - x_0}{x_1^2 - x_0^2} \right) x^2 + bx \\ & + \left[y_0 - x_0^2 \left(\frac{y_1 - y_0}{x_1^2 - x_0^2} \right) \right] \\ & + b \left[\left(\frac{x_1 - x_0}{x_1^2 - x_0^2} \right) x_0^2 - x_0 \right]. \end{aligned} \quad (A7)$$

Let us define the following constants:

$$\begin{aligned} K &= \frac{y_1 - y_0}{x_1^2 - x_0^2}, \\ L &= Kx_0^2, \\ M &= \frac{1}{x_1 + x_0}, \\ P &= Mx_0^2, \\ R &= x_0 - P, \\ A &= L - y_0. \end{aligned} \quad (A8)$$

Finally, we can represent b as

$$b = \frac{y - Kx^2 + A}{x - R - MX^2}. \quad (A9)$$

REFERENCES

- [1] L. Axel, R. C. Goncalves, and D. Bloomgarden, "Regional heart wall motion: Two-dimensional analysis and functional imaging with MR imaging," *Radiol.*, vol. 183, pp. 745–750, 1992.
- [2] H. Azhari, S. Sidman, J. L. Weiss, E. P. Shapiro, M. L. Weisfeldt, W. L. Graves, W. J. Rogers, and R. Beyar, "Three-dimensional mapping of acute ischemic regions using MRI: Wall thickening versus motion analysis," *Amer. J. Physiol.*, vol. 259, pp. H1492–H1503, 1990.
- [3] A. Azuma, "Cinevideodensitometric quantification of relative coronary arterial stenosis: Application to evaluating candidates for percutaneous transluminal coronary angioplasty," *J. Cardiol.*, vol. 19, pp. 351–363, 1989.
- [4] D. H. Ballard, "Generalizing the Hough transform to detect arbitrary shapes," *Pattern Recog.*, vol. 13, no. 2, pp. 111–122, 1981.
- [5] M. E. Bertrand, J. M. Lablanche, J. L. Fourier, G. Traisnel, and I. Mirsky, "Left ventricular systolic and diastolic function during acute coronary artery balloon occlusion in humans," *J. Amer. Coll. Cardiol.*, vol. 12, no. 2, pp. 341–347, 1988.
- [6] R. Beyar, F. C. P. Yin, M. Hausknecht, and D. Kass, "Studies of left ventricular twist in dogs and patients," in *Imaging, Analysis and Simulation of the Cardiac System*, S. Sideman and R. Beyar, Eds. London, U.K.: Freund, 1990, pp. 137–151.
- [7] V. Bhargava, "A new video intensity based wall motion analysis technique," *Comput. Med. Imag. Graphics*, vol. 14, no. 2, pp. 107–118, 1990.
- [8] C. Chen, T. Bonzel, H. Just, G. Seiffert, A. Zeiher, W. Kasper, and H. Wollschlaeger, "Quantitative assessment of temporal and spatial ventricular wall motion in normal and infarcted human left ventricles," *Amer. Heart J.*, vol. 112, no. 4, pp. 712–721, 1986.
- [9] C. Chen, J. Chou, W. Lin, and C. A. Pelizzari, "Edge and surface searching in medical images," *SPIE 914 Med. Imag. II*, pp. 594–599, 1988.
- [10] I. Deffe and Y. Neuvo, "Nonlinear zero crossing edge detection," in *Proc. 6th Scandinavian Conf. Image Anal.*, Oulu, Finland, 1989, pp. 1134–1141.
- [11] R. O. Duda and P. E. Hart, "Use of the Hough transformation to detect lines and curves in pictures," *Commun. Assoc. Comput. Machine.*, vol. 15, no. 1, pp. 11–15, 1972.
- [12] J. O. Eklundh, T. Elfving, and S. Nyberg, "Edge detection using the Marr–Hildreth operator with different sizes," in *Proc. IEEE Int. Conf. Pattern Recog.*, 1982, vol. 2, pp. 1109–1112.
- [13] R. L. Feldman, R. B. MacDonald, J. A. Hill, and C. J. Pepine, "Effect of nicardipine on determinants of myocardial ischemia occurring during acute coronary occlusion produced by percutaneous transluminal coronary angioplasty," *Amer. J. Cardiol.*, vol. 60, pp. 267–270, 1987.
- [14] T. Fukui, M. Yachida, and S. Tsuji, "Detection and tracking of blood vessels in cine-angiograms," in *Proc. IEEE 5th Int. Conf. Pattern Recog.*, Miami, FL, 1980, vol. 1, pp. 383–385.
- [15] J. J. Gerbrands, F. Booman, and H. C. Reiber, "Computer analysis of moving radiopaque markers from X-ray cinefilms," *Comput. Graphics, Image Processing*, vol. 11, pp. 35–48, 1979.
- [16] C. A. Gibbons Kroeker, J. V. Tyberg, and R. Beyar, "Effects of load manipulations, heart rate, and contractility on left ventricular apical rotation," *Circ.*, vol. 92, no. 1, pp. 130–141, 1995.
- [17] ———, "Effects of ischemia on left ventricular apex rotation: An experimental study in anesthetized dogs," *Circ.*, vol. 92, no. 12, pp. 3539–3548, 1995.
- [18] R. M. Haralick, "Zero crossing of second directional derivative edge operator," *SPIE Robot Vision*, vol. 336, pp. 91–99, 1982.
- [19] C. C. Henry and E. J. Delp, "A computer vision approach to the automatic analysis of two-dimensional echocardiograms," *Automedica*, vol. 10, pp. 49–65, 1988.
- [20] H. Ikeda, K. Shibao, M. Yoh, M. Shimamatsu, H. Shibata, K. Hiyamuta, Y. Ohkita, K. Sugi, Y. Koga, F. Utsu, and H. Toshima, "Assessment of regional wall motion abnormality without contrast medium by digital subtraction angiography using Fourier analysis," *Heart and Vessels*, vol. 1, pp. 185–186, 1985.
- [21] D. A. Kass, M. Midei, J. Brinker, and W. L. Maughan, "Influence of coronary occlusion during PTCA on end-systolic and end-diastolic pressure-volume relations in humans," *Circ.*, vol. 81, pp. 447–460, 1990.
- [22] M. J. Kern, A. Pearson, R. Woodruff, U. Deligonaul, M. Vardormael, and A. Labovitz, "Hemodynamic and echocardiographic assessment of the effects of diltiazem during transient occlusion of the left anterior descending coronary artery during percutaneous transluminal coronary angioplasty," *Amer. J. Cardiol.*, vol. 64, pp. 849–855, 1989.
- [23] N. Kiryati and A. M. Bruckstein, "Analyzing the Hough transform," *CVGIP: Graphical Models and Image Processing*, vol. 53, no. 3, pp. 213–222, 1991.

- [24] S. E. Maier, S. E. Fischer, G. C. Makinon, O. M. Hess, H.-P. Krayenbuehl, and P. Boesiger, "Acquisition and evaluation of tagged magnetic resonance images of the human left ventricle," *Comput. Med. Imag. Graphics*, vol. 16, no. 2, pp. 73–80, 1992.
- [25] V. Marangelli, S. Iliceto, and P. Rizzon, "Digital cine-loop technology: A new tool for echocardiographic evaluation of wall motion abnormalities," *Cardiologia*, vol. 35, no. 10, pp. 799–802, 1990.
- [26] M. A. Niczyporuk and D. C. Miller, "Automatic tracking and digitization of multiple radiopaque myocardial markers," *Comput., Biomed. Res.*, vol. 24, pp. 129–142, 1991.
- [27] M. Potel, J. M. Rubin, S. A. Mackay, A. M. Aisen, J. Al-Sadir, and R. E. Sayre, "Methods for evaluating cardiac wall motion in three dimensional using bifurcation points of the coronary arterial tree," *Invest. Radiol.*, vol. 18, pp. 47–57, 1983.
- [28] S. R. Ruman and J. J. Capowski, "Automated neuron tracing using the Marr–Hildreth zero crossing technique," *Comput., Biomed. Res.*, vol. 17, pp. 93–115, 1983.
- [29] A. Seit, K. Tsui, P. Nickolls, and S. Hunyor, "Use of the O2G operator in automated border extraction in echocardiographic images," *SPIE Med. Imag. II*, vol. 914, pp. 751–759, 1988.
- [30] P. W. Serruys, W. Wijns, M. van Den Brand, S. Mey, C. Slager, J. C. H. Schurbers, P. G. Huyenholtz, and R. W. Brower, "Left ventricular performance, regional blood flow, wall motion, and lactate metabolism during transluminal angioplasty," *Circ.*, vol. 70, no. 1, pp. 25–36, 1984.
- [31] T. J. Smith, Jr., W. B. Marks, G. D. Lange, W. H. Sheriff, Jr., and E. A. Neale, "Edge detection in images using Marr–Hildreth filtering techniques," *J. Neurosci. Methods*, vol. 26, pp. 75–82, 1988.
- [32] N. Srinivasa, K. R. Ramakrishnan, and K. Rajgopal, "Detection of edges from projections," *IEEE Trans. Med. Imag.*, vol. 11, no. 1, pp. 76–80, 1992.
- [33] K. S. Sunnerhagen, S. C. Smith, B. E. Jaski, and V. Bhargava, "Ischemic heart disease and regional left ventricular wall motion: A study comparing radial, central and a video intensity based slope technique," *Int. J. Cardiac Imag.*, vol. 6, pp. 85–96, 1990/1991.
- [34] D. Wohlgelemer, M. Cleman, H. A. Highman, R. C. Fetterman, J. S. Duncan, B. L. Zaret, C. C. Jaffe, "Regional myocardial dysfunction during coronary angioplasty: evaluation by two-dimensional echocardiography and 12 lead electrocardiography," *J. Amer. Coll. Cardiol.*, vol. 7, no. 6, pp. 1245–1254, 1986.
- [35] M. Yachida, M. Ikeda, and S. Tsuji, "A plan-guided analysis of cineangiograms for measurement of dynamic behavior of heart wall," *IEEE Trans. Pattern Anal. Machine Intell. PAMI*, vol. 2, no. 6, pp. 537–543, 1980.
- [36] E. A. Zerhouni, D. M. Parish, W. J. Rogers, A. Yang, and E. P. Shapiro, "Human heart: Tagging with MR imaging—A method for noninvasive assessment of myocardial motion," *Radiol.*, vol. 169, pp. 59–63, 1988.
- [37] C. A. Gibbons Kroeker, H. E. D. J. Ter Keurs, M. L. Knudtson, J. V. Tyberg, and R. Beyar, "An optical device to measure the dynamics of apex rotation of the left ventricle," *Amer. J. Physiol.*, vol. 265, pp. H1444–H1449, 1993.



Alfred M. Bruckstein was born in Transylvania, Romania, on January 24, 1954. He received the B.Sc. and M.Sc. degrees in electrical engineering, from the Technion–Israel Institute of Technology (IIT), Haifa, Israel, in 1977 and 1980, respectively, and the Ph.D. degree in electrical engineering from Stanford University, Stanford, CA, in 1984.

Since October 1984, he has been with the Technion–IIT, where he is a Professor of Computer Science. He is a frequent visitor at Bell Laboratories, Murray Hill, NJ (where he presently is on sabbatical). His research interests are in computer vision, pattern recognition, image processing, and computer graphics. He has also done work in eshmadon theory, signal processing, algorithmic aspects of inverse scattering, point processes and mathematical models in neurophysiology.

Prof. Bruckstein is a member of SIAM, MAA, and AMS.



Rafael P. Beyar (M'82) was born in Israel in 1952. He received the M.D. degree from Tel Aviv University, Tel Aviv, Israel, and obtained the D.Sc. degree in biomedical engineering from the Technion–Israel Institute of Technology (IIT), Haifa, Israel.

Since 1984, he has been with the Julius Silver Institute, Department of Biomedical Engineering, Technion–IIT. From 1985 to 1987, he was at the Division of Cardiology, Johns Hopkins University Hospital, Baltimore, MD. He was a Visiting Professor of Medicine and a Visiting Scientist to Alberta at the University of Calgary, Calgary, Alta, Canada (1991–1992). He is currently a Professor in the Department of Biomedical Engineering, Head of the Cardiac Research Center at the Technion, and Director of the Division of Invasive Cardiology, Rambam Medical Center, Haifa, Israel. His interests include modeling, simulation of the cardiovascular system, 3-D analysis of ventricular function, magnetic resonance imaging (MRI), coronary flow, coronary stems, interventional cardiology, cardio-pulmonary resuscitation (CPR), and cardiac assist. He has authored and co-authored more than 100 scientific publications and is editor of nine volumes dealing with imaging, analysis, simulation, and control of the cardiac system.

Dr. Beyar is a Member of Medical and Engineering societies and a recipient of a number of institutional and national excellence awards.



Daphna Palti-Wasserman was born in Israel in 1963. She received the B.Sc. degree from the Faculty of Electrical Engineering, and the M.Sc. degree from the Department of Biomedical Engineering, Technion–Israel Institute of Technology (IIT), Haifa, Israel. She is completing the D.Sc. degree in biomedical engineering from the Technion–IIT.

Her interests include imaging, image processing and analysis, computer vision, and their applications to the cardiac system.